

## Metabolic Profiling of Chronic Cadmium Exposure in the Rat

Julian L. Griffin,<sup>\*,†</sup> Lee A. Walker,<sup>‡</sup> Richard F. Shore,<sup>‡</sup> and Jeremy K. Nicholson<sup>†</sup>

*Biological Chemistry, Biomedical Sciences Division, The Sir Alexander Fleming Building, Exhibition Road, Imperial College of Science, Medicine and Technology, London, SW7 2AZ, U.K., and NERC Centre for Ecology and Hydrology, Monks Wood, Huntingdon, Cambridgeshire, PE28 2LS, U.K.*

Received May 2, 2001

A confounding problem with studying the effects of environmental exposure to contaminants in wild populations is that analytical techniques are invasive, particularly where the physiological effects of the toxin are assessed. In this study, a metabonomic approach to investigate the biochemical effects of chronic oral exposure to environmentally realistic doses of CdCl<sub>2</sub> (low, 8 mg/kg; high, 40 mg/kg) is presented. <sup>1</sup>H NMR spectra of urine from exposed animals were analyzed using pattern recognition methods to identify biomarkers for a 94 day exposure period. Creatinuria and both increased excretion and complexation of citrate was detected after 19 days of exposure in both exposure groups. This was accompanied by a decrease in plasma Ca<sup>2+</sup>/Mg<sup>2+</sup> ratio in blood plasma after 94 days. Post mortem, magic angle spinning (MAS) <sup>1</sup>H NMR spectroscopy was used alongside conventional analytical techniques to investigate intact tissue directly. According to atomic absorption spectroscopy, kidney tissue accumulated 26.8 ± 2.5 μg of Cd<sup>2+</sup>/g dry wt (low) and 75.9 ± 4.3 μg of Cd<sup>2+</sup>/g dry wt (high). Using high-resolution MAS <sup>1</sup>H NMR spectroscopy altered lipid content was detected in kidneys from animals exposed to Cd<sup>2+</sup>. However, unlike acute exposure, no testicular damage was evident. This systemic approach to metabolism demonstrated the different physiological effects of chronic subacute compared with an acute exposure to Cd<sup>2+</sup>.

### Introduction

Cadmium is a common contaminant of many natural environments (1–3). While its impact on human and animal health has been well studied in terms of acute and subacute exposure (4–9), effects of low-level chronic exposure, especially in the field, are poorly understood. During acute exposure, Cd<sup>2+</sup> induced necrosis and cellular damage is known to occur in kidney, liver, and testicular tissue; chronic exposure results in damage to kidneys and bone (8–11).

One of the salient problems of monitoring chronic exposure to environmental contaminants, such as Cd<sup>2+</sup>, is the lack of a suitable noninvasive technique to record tissue Cd<sup>2+</sup> accumulation and its biochemical effects. Cd<sup>2+</sup> accumulation can be monitored using atomic absorption spectroscopy of tissue extracts but this does not measure the bioactivity of the metal. Although chemical assays can record the increased expression of metallothionein following Cd<sup>2+</sup> exposure and histology can monitor nephrotoxicity, both are invasive and destructive techniques involving considerable sample preparation (4, 5, 12, 13).

The use of coupled pattern recognition (PR) and <sup>1</sup>H NMR spectroscopy of biofluids [metabonomics (14)] has proven to be a powerful technique in monitoring the toxicological effects of many compounds in both animals and man (11, 14–16). It provides information on the degree of toxicity and its mode of action. Because the

technique requires only the collection of a urine sample, it also has the advantage of being noninvasive. Previously, analysis of urine using <sup>1</sup>H NMR spectroscopy identified various biomarkers of acute Cd<sup>2+</sup> toxicity (11). It was shown that urinary creatine concentration increased as a result of testicular damage, while TCA cycle intermediates were reduced due to inhibition of renal carbonic anhydrase and subsequent alterations in TCA cycle fluxes. However, these biomarkers were the result of acute toxicity that followed intraperitoneal injection of 6–24 mg of Cd<sup>2+</sup>/kg. Exposure of wild small mammals in contaminated habitats is rarely this high and is also primarily the result of ingestion of contaminated diet and soil (7). Absorption of Cd<sup>2+</sup> across the gut lining accounts for only 3–5% of ingested Cd<sup>2+</sup> (1, 9) and so the internal dose of free living animals is much lower than that used in the Nicholson and co-workers study (11) along with other acute studies that involve intraperitoneal injection. The dynamics of organ toxicity following environmental Cd<sup>2+</sup> exposure are also expected to vary, depending upon whether exposure is acute or chronic.

In the present study, we have used a combination of PR and <sup>1</sup>H NMR spectroscopy to monitor the biochemical changes induced in laboratory rats by a 94 day exposure to environmentally realistic doses of Cd<sup>2+</sup> incorporated into their diet. At the end of the study, a range of organs were analyzed using <sup>1</sup>H NMR spectroscopy so that biochemical changes could be correlated with tissue damage. Conventional liquid-state NMR could be applied to blood plasma, but, to determine whether renal or testicular damage had occurred, high-resolution magic

\* To whom correspondence should be addressed. Phone: +(44) 020-7594-3230. Fax: +(44) 020-7594-3226. E-mail: j.griffin@ic.ac.uk.

<sup>†</sup> Biological Chemistry.

<sup>‡</sup> NERC Centre for Ecology and Hydrology.

angle spectroscopy (HRMAS)  $^1\text{H}$  NMR spectroscopy of the intact tissue was used. NMR spectroscopy of intact tissue is marred by broad resonances arising from dipole–dipole intermolecular couplings, bulk magnetic field inhomogeneities, and short  $T_2$  relaxation. However, by spinning intact tissue samples at the magic angle ( $\theta = 54.7^\circ$ ) and at speeds in excess of the dipole–dipole couplings and magnetic field inhomogeneities, high-resolution spectra, comparable to those from tissue extracts, can be obtained (17–21). Unlike extracts, all the metabolites present in a tissue sample can be examined simultaneously using this technique. This provided a holistic approach to studying the perturbations induced in systemic metabolism. These perturbations demonstrated how chronic exposure to  $\text{Cd}^{2+}$  fundamentally differs in terms of target organ toxicity and mechanism compared with an acute insult.

## Materials and Methods

**Collection of Biological Samples.** Sprague Dawley male rats (Strain, CrI, CD(SD) IGS BR, Charles River, U.K.) were kept throughout the study in standard plastic cages in a constant environment (15.5 light; 8.5 dark,  $20^\circ\text{C}$ ). They were initially fed ad libitum on standard laboratory feed (RM1; Special Diet Services, Witham, U.K.). The rats were subdivided into three groups of six, placed in separate metabolic cages and allowed to acclimatize for 24 h. Urine was then collected over ice packs for 24 h; urine collectors contained a small quantity (0.01%) of sodium azide to prevent bacterial contamination. Any food particles or faeces were removed from the urine sample by centrifugation, and the samples were stored at  $-20^\circ\text{C}$  prior to NMR analysis. These urine collections were used to provide predose measurements for all three rat groups. Subsequently, animals were maintained for 94 days on either the normal (control) diet, or the same diet with nominal concentrations of 8 (low) or 40 (high)  $\text{mg/kg}$   $\text{CdCl}_2$ . Urine samples were subsequently collected (as described above) at 6 h, 24 h, 2 days, 3 days, 9 days, 19 days, 26 days, 44 days, 58 days, 75 days, and 94 days after animals were placed on the  $\text{Cd}^{2+}$  enriched diet.

At the end of the experiment rats were sacrificed by cervical dislocation and a terminal trunk bleed was immediately collected in heparinised tubes. Blood was centrifuged at 10 000 rpm for 10 min, and the plasma separated and stored at  $-20^\circ\text{C}$ .

At post mortem any gross anatomical changes were noted visually. The left kidney was then removed within 20 s and  $\sim 20$  mg sections were taken from the inner renal cortex and papilla for HRMAS spectroscopy. The right kidney was removed for  $\text{Cd}^{2+}$  analysis by atomic absorption spectroscopy (see below). About 20 mg of testicular tissue (general tubular region) was removed and analyzed by HRMAS spectroscopy. Samples of liver were also removed to determine metallothionein concentration (see below). All tissues were snap-frozen in liquid nitrogen immediately after dissection and stored at  $-70^\circ\text{C}$  prior to analysis.

**NMR Spectroscopy of Urine and Blood Plasma.**  $^1\text{H}$  NMR spectra were obtained on a Bruker Avance DRX-600 Spectrometer operating at 600.13 MHz  $^1\text{H}$  frequency at 298 K. Urine samples were examined using a broad band inverse-detected flow injection probe operated using the BEST automation package (Bruker, Germany). Each urine sample consisted of 600  $\mu\text{L}$  of urine, 300  $\mu\text{L}$  of sodium phosphate buffer (pH 7.1), and 100  $\mu\text{L}$  of  $\text{D}_2\text{O}$  (internal lock) with TSP (final concentration 1 mM) as an internal reference standard ( $\delta = 0$  ppm).  $^1\text{H}$  NMR spectra were collected using a selective solvent presaturation sequence with 32 scans, an acquisition time of 2.34 s and a further relaxation delay of 5 s (22). The spectra were acquired using 7 kHz spectral width and 32k time domain data points.

Spectra were Fourier transformed following multiplication of an exponential term equivalent to 0.3 Hz line broadening.

Resonances from key metabolites were integrated using standard Bruker software (XWIN NMR version 2.5).

Blood plasma was also analyzed by  $^1\text{H}$  NMR spectroscopy using both the conventional solvent presaturation pulse sequence described above (128 scans) and a Carr-Purcell-Meiboom-Gill (CPMG) spin-echo experiment ( $(90 - (\tau-180-\tau))_n - \text{acquisition}$ ) as a  $T_2$  filter to attenuate broad signals from proteins and lipoproteins (22). CPMG spectra were acquired with 256 scans with a total spin-spin ( $T_2$ ) relaxation delay of 80 ms, and an interpulse delay of 2 s. Other acquisition parameters were as described above. Each plasma sample consisted of 400  $\mu\text{L}$  of plasma diluted by 400  $\mu\text{L}$  of  $\text{D}_2\text{O}$  containing 1 mM TSP and 5 mM EDTA. EDTA was added to assess the cation content of the blood plasma samples (23).

**MAS  $^1\text{H}$  NMR Spectroscopy Analysis of Renal Tissue.** HRMAS  $^1\text{H}$  NMR spectra were collected on 600 MHz Bruker DRX spectrometers using a modified CPMG spin-echo pulse sequence to remove the effects of lipids and large macromolecules on spectral broadening ( $n = 20$ ; total spin-spin relaxation delay ( $2n\tau$ ) = 40 ms; relaxation delay = 2 s between pulses). Samples ( $\sim 20$  mg) were spun at 5000 Hz at the magic angle ( $54.7^\circ$ ) in the presence of  $\text{D}_2\text{O}$  to provide a deuterium lock. For both renal and testicular tissue, spectra were acquired with 256 scans into 32k data points with a spectral width of 4807.7 Hz and a total pulse recycle delay of 9.82 s.

**$\text{Cd}^{2+}$  Concentrations in Renal Tissue.** Samples were dried at  $80^\circ\text{C}$  to constant weight, cold digested in 0.5 mL concentrated nitric acid (Analar grade; BDH, Poole, U.K.), and then hot digested at  $120^\circ\text{C}$  until completely solubilized. Two 0.2 mL aliquots of 30% w/v hydrogen peroxide (BDH, U.K.) were added during digestion to aid sample oxidation. Digests were diluted and analyzed by flame atomic absorption spectroscopy (Solar 969, Thermo Unicam, Cambridge, U.K.). The mean ( $\pm$ SE) % recovery from a certified reference material (Reference material 186, Community Bureau of Reference) was  $83.5 \pm 2.29\%$  ( $n = 3$ ) and recoveries from two spiked blanks and four spiked tissue samples were 104–110 and 109–121%, respectively. The limit of detection (LoD) in the hepatic and renal samples (based on mean sample weights) were 0.41 and 3.22  $\mu\text{g}$  of  $\text{Cd}^{2+}$ /g dry weight (dw) respectively, while the LoD for the diet samples was 2.77  $\mu\text{g}$  of  $\text{Cd}^{2+}$ /g wet weight (ww).

**Metallothionein Content in Hepatic Tissue.** Hepatic metallothionein residues were determined by cadmium-saturation (24). Liver samples were homogenized in 0.25 M sucrose in Tris-HCl buffer (pH 7.5) and centrifuged at  $4^\circ\text{C}$ . The supernatant was removed and the metallothionein present saturated with  $\text{CdCl}_2$ . Excess  $\text{Cd}^{2+}$  was then removed by binding with haemoglobin (2% w/v bovine haemoglobin; Sigma, Poole U.K.) solution, which was then denatured by heat treatment and removed from the sample by centrifugation. The samples were then acidified with nitric acid and the  $\text{Cd}^{2+}$  content of the acidified sample determined by flame-atomic absorption spectroscopy. The concentration of metallothionein in the liver was calculated, assuming that 6  $\text{Cd}^{2+}$  bind per metallothionein protein which has a molecular weight of 6050 (25). The LoD for metallothionein in the liver samples was 3.91  $\mu\text{g}$  of protein/g tissue ww. Metallothionein concentrations in blanks included with the unknowns were below the LoD.

**Pattern Recognition Investigation of NMR Spectra.** For the purposes of pattern recognition analysis,  $^1\text{H}$  NMR spectra were data reduced (AMIX v.2 program, Bruker, Germany) by being sub-divided into 0.04 ppm designated regions from  $\delta$  0.4–10.0 for urine and  $\delta$  0.4–4.5 for blood plasma and MAS spectra (15, 26, 27). The residual water peak area was excluded from analysis and then the area of the resonances within each remaining region integrated. Each spectral region was normalized to the summation of spectral regions for the entire spectrum, which accounted for dilution or bulk mass differences between samples. Correlation Principal Components Analysis (PCA) was performed using Pirouette v. 2.6 (InfoMetrix, Woodinville, WA). PCA is an unsupervised method of classification, requiring no training set of data, that mathematically correlates

**Table 1. Mean Concentrations of Cadmium in the Diets ( $\mu\text{g}$  of  $\text{Cd}/\text{g}$  of ww), Renal, and Hepatic Tissues (both  $\mu\text{g}$  of  $\text{Cd}/\text{g}$  of dw) and Hepatic Metallothionein Residues ( $\mu\text{g}$  of MT/ $\text{g}$  of ww) for Rats Fed Control, Low ( $8 \mu\text{g}$  of  $\text{Cd}^{2+}/\text{g}$ ) and High ( $40 \mu\text{g}$  of  $\text{Cd}^{2+}/\text{g}$ ) Cadmium-Contaminated Diets<sup>a</sup>**

treatment	Cd in diet	renal Cd	hepatic Cd	hepatic MT
control	<2.77	<3.22	<0.4	<3.9
low Cd	$8.8 \pm 0.3$	$26.8 \pm 2.5$	$3.0 \pm 0.3$	$13.2 \pm 1.7$
high Cd	$35.7 \pm 1.65$	$75.9 \pm 4.3$	$8.9 \pm 1.1$	$31.0 \pm 2.9$

<sup>a</sup>  $N = 6$  for dietary, renal and hepatic Cd concentration, and  $N = 5$  for hepatic MT residues.

the variation detected in a data set to a spatial representation of the data. The first PC generated by this method represents the maximum variation that can be correlated together for the data. Subsequent PCs represent less variation and are chosen to be orthogonal to the first PC.

Both mean-centered and autoscaling routines were applied to the spectral data prior to independent PCA. Mean-center analysis involved subtraction of the mean of the integral for a designated spectral region and measures variance about this mean. Thus, PCs in mean centered data are influenced by regions with the maximum variance about the mean. Autoscaled analysis sets each integral region to unit variance, ensuring the sum of a single PC across all observables will be zero. This weights spectra so that features with lower spectral intensity and the high concentration metabolites contribute equally to the PC analysis. Spectral data were reduced from 240 spectral descriptors to a number of PCs (less than 5) as determined by the maximization of cumulative total variation in the data that is predicted by those components. Loading plots from the PC analysis were used to identify resonances to predict metabolite changes within renal tissue exposed to  $\text{Cd}^{2+}$ . These predictions were then cross validated with spectra both visually and by manual integration of the regions.

**Statistical Analysis.** Data are represented as means  $\pm$  standard error of the mean. Students *t*-test and Tukey tests were performed using Instat (Graphpad Inc, CA).

## Results

**$\text{Cd}^{2+}$  Accumulation and Metallothionein Expression.** Rats fed either diet contaminated with  $\text{CdCl}_2$  accumulated  $\text{Cd}^{2+}$  in both renal and hepatic tissue (Table 1). The  $\sim 4$ -fold increase in the mean  $\text{Cd}^{2+}$  concentrations from the low to high cadmium contaminated diets corresponded to a difference in both renal and hepatic  $\text{Cd}^{2+}$  concentrations of  $\sim 3$ -fold. Increased metallothionein expression was also detected in hepatic tissues from rats fed the contaminated diets, with a  $\sim 2$ -fold increase in expression between the high and low dose exposure groups (Table 1).

**NMR Spectroscopy of Urine Demonstrates Creatinuria and Cation Chelation by Citrate.** The  $^1\text{H}$  NMR urinary profiles (Figure 1) were analyzed by PR to determine the metabolic consequence of  $\text{Cd}^{2+}$  insult across the time course. Separation of some urine profiles from the cluster of control spectra was apparent from 19 days for animals in the high dose group and three animals from the low dose group for both mean centered and autoscaled PC analysis (Figure 2). The separation was more evident following mean centered analysis indicating the metabolites correlated most to cadmium toxicity were caused by high concentration metabolites. The separation was caused by four effects: an increase in sugars, an increase in creatine, a decrease in hippurate and a low-frequency shift in the chemical shift of the citrate resonance (Figure 1). While at no time point was

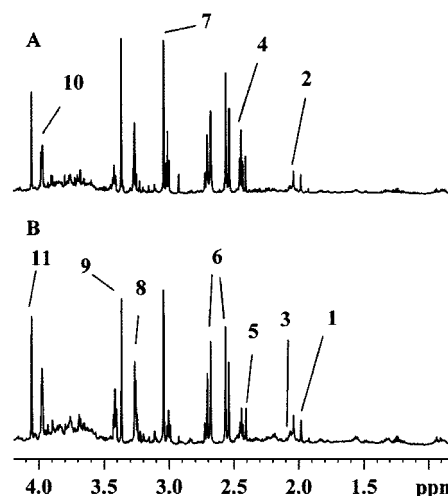


**Figure 1.** Urinary profiles from control (A) and high dose (B)  $\text{CdCl}_2$  (40 ppm) exposed rats after 19 days of exposure. Key: 1, acetate; 2, acetylated glycoproteins; 3, glutamate; 4,  $\alpha$ -ketoglutarate; 5, oxaloacetate; 6, citrate; 7, creatine/creatinine; 8, phosphocholine and taurine (underlying triplet); 9, trimethylamine-*N*-oxide; 10, creatine; 11, creatinine.

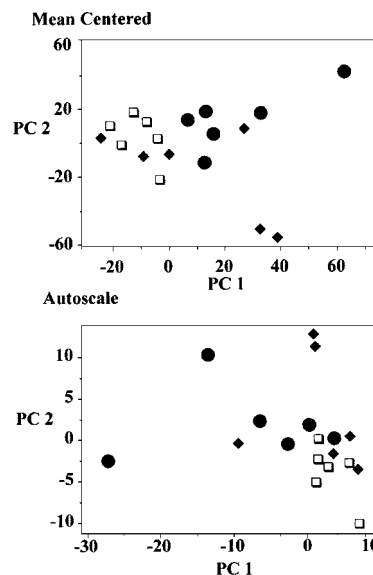


**Figure 2.** Mean centered and autoscaled preprocessing PC analysis of urinary profiles at 19 days of exposure to  $\text{CdCl}_2$  in feed. Key: ( $\square$ ) control, ( $\blacklozenge$ ) low dose (8 ppm), ( $\bullet$ ) high dose.

complete separation apparent for all the high, medium, and control dosed animals, at subsequent time points the majority of spectra ( $>3$ ) from both the high and medium dosed groups could be shown to occupy separate PC space compared with the remainder of the spectra. Furthermore, all the animals exposed to high and low doses of  $\text{Cd}^{2+}$  did not cluster with the control group for at least one time point. Mean PC loadings for each time point showed that the animals exposed to high and low doses of  $\text{Cd}^{2+}$  occupied a different PC space than the control cluster (Table 2). Inspection of the metabolites that contributed to the PC loadings indicated that both citrate and creatine contributed to this separation. Between 19 days and 58 days, separation occurred in either PCs 1, 2, or 3, but, after this time period, higher order PCs, which represented less of the total variation described in the spectra were the only ones that separated the groups.



**Table 2. Principle Components that Cause Clustering of Cd<sup>2+</sup> Dosed Rats in Separate PC Space to that of Controls<sup>a</sup>**

time/days	PC(s) causing separation	percentage variance of PC(s)	mean loading of PC	metabolites contributing
(A) Mean Centered				
19	PC1	35	high: 10.7 ± 6.30** low: 8.7 ± 4.8** control: -20.6 ± 1.38	citrate (+); creatine (+); taurine (-)
26	PC4	7.5	high: -0.56 ± 1.34 low: -2.80 ± 3.26 control: 4.57 ± 1.93	creatine (+); citrate (chemical shift and +); hippurate (-)
44	PC1/PC4	50.3	high: -4.70 ± 2.00** low: -1.42 ± 1.15* control: 5.35 ± 1.62	citrate (chemical shift); creatine (+)
58	PC3	13.5		creatine (+); citrate (chemical shift and +); taurine (-)
75	no separation	7.2		citrate (chemical shift); creatine (+); hippurate (+)
96	PC4/PC5			
(B) Autoscale				
19	PC2	21.1	high: 0.21 ± 1.88 low: 3.64 ± 2.03 control: -2.50 ± 0.98	creatine (+); lactate (+); hippurate (-); taurine (-); glutamate (+); leucine (+), isoleucine (+); valine (+)
26	no separation	26.3		sugars/glucose (+); lactate (+); glutamate (+); hippurate (-); taurine (-)
44				
58	PC1	32.5	high: 2.28 ± 2.56 low: 4.55 ± 2.74* control: -5.64 ± 2.50	creatine (+); citrate (chemical shift and +). sugars (+); low concentrated aromatic amino acids (+)
75	PC2/PC4	29.3	high: 1.83 ± 1.13* low: 0.51 ± 1.10 control: -1.88 ± 0.62	creatine (+), sugars (+); glutamate (+); citrate (chemical shift and +)
96	PC5	3.8		creatine (+); glutamate (+); sugars/glucose (+); phenylalanine (-); tyrosine (-)

<sup>a</sup> PCs are listed for the different time points where clustering was evident along with the amount of spectral variation represented (%) by the PC and the main constituents of the PC for both autoscale and mean centered analysis. Mean ( $\pm$ SE) PCs for an exposure group have been calculated where separation was predominantly across one PC. (\*)  $p < 0.05$ , (\*\*)  $p < 0.005$  for significant difference from control group.

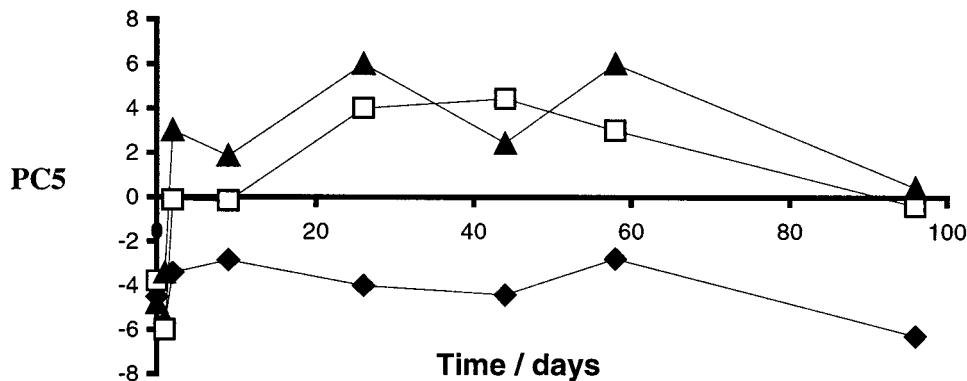


**Figure 3.** Plot of PC5 versus time for three animals exposed to either a diet containing no (◆), low (□), or high Cd<sup>2+</sup> (▲). Time points plotted at predose (-1 day), 1, 2, 19, 26, 44, 58, and 94 days. Other time points omitted due to changes in solvent suppression quality across the spectra.

To investigate further the temporal variance in urinary profiles, the mean spectral profile (a summation of the spectra for each individual in a treatment group) were analyzed using mean centered PCA across the majority of time points (time points where data had bad water suppression were excluded from this analysis). This demonstrated that the high and low Cd<sup>2+</sup> dosed animals were most affected between 26 and 58 days after initial exposure (Figure 3). This was largely due to a change in the chemical shift and relative intensity of the citrate resonances at  $\delta$  2.58 and 2.70.

To confirm the occurrence of creatinuria in Cd-dosed animals after 19 days, the concentration of creatine was quantified by comparing the singlet resonance at  $\delta$  3.02 with two easily quantifiable metabolite resonances: acetate (singlet  $\delta$  1.91; invariant in urine between the three

groups) and taurine (triplet  $\delta$  3.41; decreased in urine of animals exposed to Cd<sup>2+</sup>). The ratio of creatine/acetate was not significantly different (high Cd<sup>2+</sup> exposed =  $4.54 \pm 0.20$ ; low Cd<sup>2+</sup> =  $4.01 \pm 0.20$ ; control =  $3.84 \pm 0.30$ ) but the creatine/taurine ratio was increased in Cd-dosed animals (high Cd<sup>2+</sup> exposed =  $3.26 \pm 0.48^{*}$ ; low Cd<sup>2+</sup> exposed =  $3.40 \pm 0.62^{*}$ ; control =  $1.63 \pm 0.22$ ; \* $p < 0.05$  for difference from control group).

The chemical shift change recorded for citrate in animals exposed to Cd<sup>2+</sup> may have been produced either by an alteration in pH or as a result of chelation of cations by the citrate. However, all urine samples were buffered to a pH of  $\sim 7.1$  and this was confirmed for the urine samples in question. To determine whether chelation was responsible for the chemical shift alteration, 5 mM EDTA was added to the 19 day urine samples. EDTA behaves

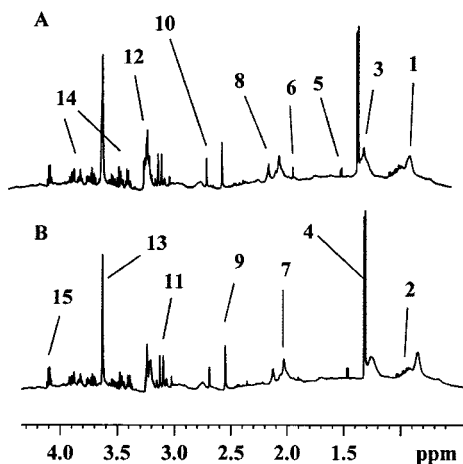


**Figure 4.** CPMG  $^1\text{H}$  NMR spectra of blood plasma from rats fed control diet (A) or diet contaminated with 40 ppm  $\text{CdCl}_2$  (B). Key: 1, VLDL and LDL  $\text{CH}_3$ -lipid groups; 2, leucine, valine, and isoleucine resonances; 3, VLDL and LDL  $\text{CH}_2\text{CH}_2\text{CH}_2$  lipid groups; 4, lactate; 5, alanine; 6, acetate; 7,  $\text{CH}_2\text{C}=\text{C}$  lipid resonances and glycoproteins; 8, methionine; 9,  $[\text{Ca-EDTA}]^{2-}$  (ethylenic protons); 10,  $[\text{Mg-EDTA}]^{2-}$  (ethylenic protons); 11,  $[\text{Ca-EDTA}]^{2-}$  (acetate protons); 12, free  $\text{EDTA}^{4-}$  and  $[\text{Mg-EDTA}]^{2-}$  (acetate protons); 13, free  $\text{EDTA}^{4-}$ ; 14, glucose resonances; 15, lactate.

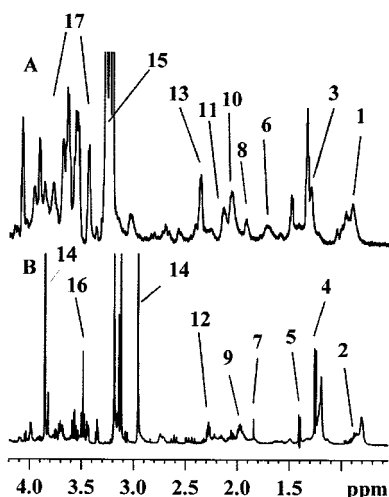


**Figure 5.** High resolution MAS  $^1\text{H}$  spectra of renal tissue (inner cortex) (A) and testicular tissue (B) from a rat exposed to a diet containing 40 ppm  $\text{CdCl}_2$ . 1,  $\text{CH}_3$  lipid groups; 2, leucine, isoleucine, and valine; 3,  $\text{CH}_2$  lipid groups; 4, lactate; 5, alanine; 6,  $\text{CH}_2\text{CH}_2\text{CO}$  lipid; 7, acetate; 8,  $\text{CH}_2\text{C}=\text{C}$  lipid; 9, glutamate; 10,  $\text{CH}_2\text{C}=\text{C}$  lipid + glutamate; 11,  $\text{CH}_2\text{C}=\text{C}$  lipid + glutamate + glutamine; 13,  $\text{CH}_2\text{CO}$ ; 14, creatine; 15, choline resonances (choline, phosphocholine, and phosphatidylcholine); 16, glycine; 17, glucose resonances.

as a competitive chelation agent and caused the citrate resonances to move to low frequencies, confirming that the shift in citrate was caused by metal complexation.

**Altered Biochemistry in Blood Plasma and Kidney Tissue, But Not in the Testes.** Blood plasma (spiked with EDTA to investigate cation content; Figure 4) and samples of renal (inner cortex and papillar; Figure 5a) and testicular tissue (Figure 5b) were examined by MAS  $^1\text{H}$  NMR spectroscopy to investigate organ toxicity. CPMG spectra of blood plasma were examined by PC analysis. Both high and low dose groups readily separated from the control group along PC2 (Figure 6), caused by decreases in the resonance intensity of  $(\text{CH}_2)_n$  lipoproteins ( $\delta$  1.33), acetate ( $\delta$  1.94) and alanine ( $\delta$  1.44). There was also an increase in intensity of the EDTA

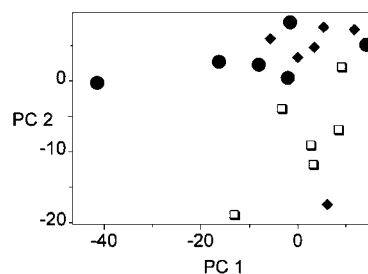


**Figure 6.** Mean centered analysis of blood plasma profiles following 94 days of exposure to  $\text{CdCl}_2$ . Key: ( $\square$ ) control, ( $\bullet$ ) low dose (8 ppm), ( $\blacklozenge$ ) high dose.

resonances at  $\delta$  3.11. Cadmium exposed rats had increased complexed  $\text{Ca}^{2+}$ :  $\text{Mg}^{2+}$  ratio compared with control rats (singlets at  $\delta$  2.61 and 2.75, respectively, control =  $1.12 \pm 0.03$ ; low =  $1.16 \pm 0.05$ ; high =  $1.51 \pm 0.06$ ;  $p < 0.001$  for difference between control and high dose and low and high dose groups). Exposure of rats to  $\text{Cd}^{2+}$  also affected the spectra obtained from both the inner cortex and the papilla of the kidney. Renal tissue from  $\text{Cd}^{2+}$  exposed animals had decreased resonance intensities for  $\text{CH}_3$  lipid triglycerides and phosphocholine but increased resonance intensities from sugars, choline, and phosphatidylcholine/inositol, as determined using PR and visual inspection of the integral regions (data not shown). Exposure to  $\text{Cd}^{2+}$  had no biochemical effect in HRMAS spectra of testicular tissue. To confirm that there was no change in the creatine content of testicular tissue in the high dose rats, the resonance of creatine ( $\delta$  3.04) was integrated along with that of choline ( $\delta$  3.20; assumed to remain constant). The ratio of testicular creatine/choline was the same for  $\text{Cd}^{2+}$  exposed and control animals (high dose  $\text{Cd}^{2+}$  exposed =  $2.7 \pm 0.5$ ; control =  $2.2 \pm 0.2$ ). To examine the redox potential of the tissue, the ratio of alanine to lactate was estimated by comparing the ratio of the resonances at  $\delta$  1.44 and 1.33, respectively; again exposure to  $\text{Cd}^{2+}$  had no detectable effect (high dose  $\text{Cd}^{2+}$  exposed =  $3.1 \pm 0.6$ ; control =  $3.4 \pm 0.4$ ).

## Discussion

Acute  $\text{Cd}^{2+}$  toxicity has been well documented both in laboratory animals and man (1–3), but subacute chronic exposure to the metal is still poorly understood. This is despite environmental exposure to  $\text{Cd}^{2+}$  most commonly involving long term chronic exposure, rather than an acute incident. In the present study, we used urinary profiles to metabolically profile the changes in systemic biochemistry during chronic exposure to  $\text{Cd}^{2+}$ . These changes were cross-correlated with evidence for toxicity within organs targeted by  $\text{Cd}^{2+}$ . Chronic exposure to  $\text{Cd}^{2+}$  both induced different biochemical processes within tissues and targeted different organs compared with acute toxicity.

Creatinuria was one of the major impacts of  $\text{Cd}^{2+}$  insult during high and low dose chronic exposure. This was detected by pattern recognition and confirmed in terms of crude metabolite ratios (creatinine/taurine ratio). Elevated urinary creatine is also the dominant feature of acute  $\text{Cd}^{2+}$  toxicity in male rats (22, 28, 29) and is caused by testicular atrophy from vascular constriction (22), although  $\text{Cd}^{2+}$  toxicity in the testes may also affect testicular tissue directly (30). However, in the present study, there was no reduction in creatine in the testes of

rats exposed chronically to either high or low  $\text{Cd}^{2+}$  doses. Furthermore, the redox potential of testicular tissue was similar between  $\text{Cd}^{2+}$  exposed tissue and control tissue, demonstrating that testicular toxicity had not occurred. There was also no evidence of reduced creatine content in renal tissue. Thus, another source of creatine must have been responsible for the creatinuria detected after 19 days of exposure.

A principal feature of acute  $\text{Cd}^{2+}$  toxicity is renal tubular acidosis. This is caused by direct inhibition of carbonic anhydrase (11). Without carbonic anhydrase to modulate renal pH, the kidney consumes glutamine to generate  $\text{NH}_4^+$  ions and so modulates pH (31–33). This is accompanied by a reduction in renal glutamate content, as previously observed in the renal tissue of bank voles (*Clethrionomys glareolus*) (9). While no change in glutamate content was detected in rat renal tissue in the present study, a requirement by the kidney for glutamine would explain the urine creatinuria detected. Muscle is rich in both glutamine and creatine and the tissue exports glutamine to stimulate other organs, particularly the kidney, during pH regulation (31, 32). This process impairs muscular metabolism, and may have caused the transient creatinuria detected in this study. Creatinuria was less marked later in the study, and no excess of creatine or glutamine was detected in blood plasma. However, a reduction in blood plasma alanine was detected in rats exposed to the high dose of  $\text{Cd}^{2+}$ , and a combination of alanine amino transferase and glutamate dehydrogenase could supply renal tissue with  $\text{NH}_4^+$  ions to reduce the effects of  $\text{Cd}^{2+}$  induced long-term renal acidosis. This demonstrates that, while acute toxicity causes transient renal acidosis, systemic metabolism is altered during chronic exposure to maintain normal renal function.

A transient increase in citrate excretion, and a change in the chemical shift of four resonances of the molecule were detected in high and low dose exposed rats. Nicholson and co-workers (11) previously found that acute exposure to  $\text{Cd}^{2+}$  caused a decrease in citrate concentration, as well as other TCA cycle intermediates. This was caused by a decrease in TCA cycle flux following renal tubular acidosis. The changes seen in the present study following chronic exposure to  $\text{Cd}^{2+}$  are fundamentally different. The chemical shift change of the citrate resonances was not induced by urine acidosis, but by chelation of ions by citrate.  $\text{Cd}^{2+}$  displaces  $\text{Ca}^{2+}$  within the body (2) and an increase in extracellular free  $\text{Ca}^{2+}$  is detrimental to renal tissue as excess calcium precipitates as calcium phosphate. The decrease in taurine urinary excretion that was detected also indicates that there was a change in osmoregulatory homeostasis, as taurine is a known osmoregulatory compound. Increased  $\text{Ca}^{2+}$  content, compared with  $\text{Mg}^{2+}$  plasma concentration, was also detected in blood plasma samples, which is consistent with  $\text{Cd}^{2+}$ -induced displacement of tissue  $\text{Ca}^{2+}$ .

In rats exposed to the high dose of  $\text{Cd}^{2+}$ , renal tissue had decreased  $\text{CH}_3$  lipid but increased choline/phosphocholine content. We have previously demonstrated an alteration in the lipid profile of bank voles chronically exposed to the high  $\text{Cd}^{2+}$  diet for 14 days (26). This was thought to have been caused either by a necrosis-induced change in cell populations, infiltration of immune cells to repair damaged renal tissue, or mitochondrial proliferation, which is known to accompany chronic  $\text{Cd}^{2+}$  exposure in both birds and laboratory mice (5). However,

a decrease in  $\text{CH}_3$  lipids was detected in blood plasma in this study, indicating that some of the lipid profile changes were caused by alterations in lipid and fatty acid transport. While the kidney is the primary site of  $\text{Cd}^{2+}$  storage, the liver also accumulates significant amounts of the metal (Table 1; refs 1, 2, 8, 9, 34). Hepatic tissue stores and modifies lipids, and reductions of  $\text{CH}_3$  lipid moieties in blood plasma and the kidneys may indicate hepatic damage.

Two exposure levels were used during this study, with the higher dose being four times larger than the lower. However, accumulation of  $\text{Cd}^{2+}$  within renal and hepatic tissue only increased 3-fold. Furthermore, metallothionein expression only increased 2-fold. This suggests that at higher exposure levels,  $\text{Cd}^{2+}$  is either stored peripherally to the kidney and liver, or excretory mechanisms are increased. This emphasizes again the difference in pathology induced by acute and chronic cadmium toxicity. While acute exposure to cadmium causes the metal to be rapidly accumulated within liver and kidney tissue, the burden of chronic exposure is reduced in these two tissues.

In this study, we have recorded the physiological effects of a subacute, chronic exposure to  $\text{Cd}^{2+}$  toxicity. Unlike acute exposure to the metal, the vascular system of the testes was not targeted. While renal metabolism is perturbed in both acute and chronic exposure, adaptive mechanisms counteract renal tubular acidosis during chronic exposure. This is not the case following acute exposure. However, following chronic exposure the kidney is also affected by an alteration in lipid content, possibly caused by mitochondrial proliferation. Analysis of both blood plasma and urine indicated that there was a perturbation in systemic metabolism caused by chronic exposure.

In conclusion, our study clearly demonstrates the very different effects that a contaminant may have depending upon whether exposure is either acute or chronic. The consequences are that different organs are targeted, and different biochemical pathways within the affected tissue are induced. The results have clear implications about the potential pitfalls in extrapolating the results of acute exposure studies to environmental situations, and demonstrate the ease of a "metabonomics" approach to following environmental toxicology.

**Acknowledgment.** This work was supported by an Environmental Diagnostic award made by the Natural Environment Research Council, UK. J.L.G. is a Royal Society University Research Fellow.

## References

- (1) Bremner, I. (1979) *The Chemistry, Biochemistry and Biology of Cadmium* (Webb, M., Ed.) pp 175–193, Elsevier, Amsterdam.
- (2) Goyer, R. A. (1995) in *Casarett and Doull's Toxicology* (Klassen, C. D., Ed.) 5th ed., pp 699–702, McGraw-Hill Professional Publishing, Singapore.
- (3) Peterson, A. P., and Alloway, B. J. (1979) *The Chemistry, Biochemistry and Biology of Cadmium* (Webb, W., Ed.) pp 45–92, Elsevier, New York.
- (4) Nicholson, J. K., Kendall, M. D., and Osborn, D. (1983) Cadmium and mercury nephrotoxicity. *Nature* **304**, 633–635.
- (5) Nicholson, J. K., and Osborn, D. (1983) Kidney lesions in pelagic seabirds with high tissue levels of cadmium and mercury. *J. Zool. London* **200**, 99–118.
- (6) Roels, H., Bernard, A., Buchet, J. P., Goret, A., Lauwerys, R., Chettle, D. R., Harvey, T. C., and Haddad, I. A. (1979) Critical concentration of cadmium in renal cortex and urine. *Lancet* **1**, 221.

- (7) Shore, R. F., and Douben, P. E. T. (1994) The ecotoxicological significance of cadmium intake and residues in terrestrial small mammals. *Ecotoxicol. Environ. Saf.* **29**, 101–112.
- (8) World Health Organisation (1980) *Recommended Health-Based Limits in Occupational Exposure to Heavy Metals*, WHO, Geneva.
- (9) World Health Organisation (1992) *Environmental Health Criteria 134: Cadmium*, WHO, Geneva.
- (10) Dunnick, J., and Fowler, B. A. (1988) in *Handbook on Toxicity of Inorganic Compounds* (Seller, H. G., and Siegel, H., Eds.) pp 115–174, Marcel Dekkar, New York.
- (11) Nicholson, J. K., Hingham, D. P., Timbrell, J. A., and Sadler, P. J. (1989) Quantitative high resolution  $^1\text{H}$  NMR Urinalysis studies on the biochemical effects of cadmium in the rat. *Mol. Pharmacol.* **36**, 398–404.
- (12) Larison, J. R., Likens, G. E., Fitzpatrick, J. W., and Crock, J. G. (2000) Cadmium toxicity among wildlife in the Colorado Rocky Mountains. *Nature* **411**, 181–183.
- (13) Richardson, M. E., Fox, M. R., and Fry, B. E. (1973) Pathological changes produced in Japanese Quail by ingestion of cadmium. *J. Nutr.* **104**, 323–338.
- (14) Nicholson, J. K., Lindon, J. C., and Holmes, E. (1999) 'Metabonomics': understanding the metabolic responses of living systems to pathophysiological stimuli via multivariate statistical analysis of biological NMR data. *Xenobiotica* **11**, 1181–1189.
- (15) Anthony, M. L., Sweatman, B. C., Beddell, C. R., Lindon, J. C., and Nicholson, J. K. (1994) Pattern recognition classification of the site of nephrotoxicity based on metabolic data derived from proton nuclear magnetic resonance spectra of urine. *Mol. Pharmacol.* **46**, 199–211.
- (16) Holmes, E., Nicholls, A. W., Lindon, J. C., Ramos, S., Spraul, M., Neidig, P., Connor, S. C., Connelly, J., Damment, S. J., Haselden, J., and Nicholson, J. K. (1998) Development of a model for classification of toxin-induced lesions using  $^1\text{H}$  NMR spectroscopy of urine combined with pattern recognition. *NMR Biomed.* **11**, 235–244.
- (17) Andrew, E. R., and Eades, R. G. (1959) Removal of dipolar broadening of NMR spectra of solids by specimen rotation. *Nature* **183**, 1802.
- (18) Cheng, L. L., Ma, M. J., Becerra, L., Hale, T., Tracey, I., Lackner, A., and Gonzalez, R. G. (1997) Quantitative neuropathology by high-resolution magic angle spinning proton magnetic resonance spectroscopy. *Proc. Natl. Acad. Sci. U.S.A.* **94**, 6408–6413.
- (19) Garrod, S., Humpfer, E., Spraul, M., Connor, S. C., Polley, S., Connelly, J., Lindon, J. C., Nicholson, J. K., and Holmes, E. (1999) High-resolution MAS- $^1\text{H}$  NMR spectroscopic studies on intact rat renal cortex and medulla. *Magn. Reson. Med.* **41**, 1108–1118.
- (20) Millis, K., Maas, E., Cory, D. G., and Singer, S. (1997) Gradient high-resolution magic angle spinning nuclear magnetic resonance spectroscopy of human adipocyte tissue. *Magn. Reson. Med.* **38**, 399–403.
- (21) Millis, M., Weybright, P., Campbell, N., Fletcher, J. A., Fletcher, C. D., Cory, D. G., and Singer, S. (1999) Classification of Human Liposarcoma and Lipoma using Ex vivo Proton NMR spectroscopy. *Magn. Res. Med.* **41**, 257–267.
- (22) Nicholson, J. K., Foxall, P. J., Spraul, M., Farrant, R. D., and Lindon, J. C. (1995) 750 MHz  $^1\text{H}$  and  $^1\text{H}$ - $^{13}\text{C}$  NMR spectroscopy of human blood plasma. *Anal. Chem.* **67** (5), 793–811.
- (23) Nicholson, J. K., Buckingham, M. J., and Sadler, P. J. (1983) High resolution  $^1\text{H}$  nmr studies of vertebrate blood and plasma. *Biochem. J.* **211**, 605–615.
- (24) Onaka, S., and Cherian, M. G. (1982) Comparison of metallothionein Determination by polarographic and cadmium-saturation methods. *Toxicol. Appl. Pharmacol.* **63**, 270–274.
- (25) Kagi, J. H. R., and Vallee, B. L. (1961) Metallothionein: a cadmium and zinc containing protein from equine renal cortex. II. Physicochemical properties. *J. Biol. Chem.* **236**, 2435–2442.
- (26) Griffin, J. L., Walker, L. A., Troke, J., Osborn, D., Shore, R. F., and Nicholson, J. K. (2000) The initial pathogenesis of cadmium induced renal toxicity. *FEBS Lett.* **478**, 147–150.
- (27) Holmes, E., Nicholls, A. W., Lindon, J. C., Ramos, S., Spraul, M., Neidig, P., Connor, S. C., Connelly, J., Damment, S. J., Haselden, J., and Nicholson, J. K. (1998) Development of a model for classification of toxin-induced lesions using  $^1\text{H}$  NMR spectroscopy of urine combined with pattern recognition. *NMR Biomed.* **11**, 235–244.
- (28) Gunn, S., Gould, T. C., and Anderson, W. (1982) The selective injurious response of testicular and epididymal blood vessels to cadmium and its prevention by zinc. *Am. J. Pathol.* **42**, 685–696.
- (29) Samarickmansinghe, G. P. (1979) Biological effects of cadmium in mammals. In *The Chemistry, Biochemistry and Biology of Cadmium* (Webb, M., Ed.) Elsevier/North-Holland Biomedical Press, Amsterdam.
- (30) Janecki, A., Jakubowiak, A., and Steinberger, A. (1992) Effect of Cadmium Chloride on Transepithelial Electrical Resistance of Sertoli Cell Monolayers in Two-Compartment Cultures. *Toxicol. Appl. Pharmacol.* **112**, 51–57.
- (31) Hems, D. A. (1972) Metabolism of glutamine and glutamic acid by isolated perfused kidneys of normal and acidotic rats. *Biochem. J.* **130**, 671–680.
- (32) Newsholme, E. A., and Leech, A. R. (1983) *Biochemistry for the Medical Sciences*, p 512, Wiley, London.
- (33) Goldstein, L. (1980) Adaptation of renal ammonia production to metabolic acidosis. *The Physiologist* **23**, 19–25.
- (34) Shore, R. F., Myhill, D. G., Routledge, E. J., and Wilby, A. (1995) Impact of an environmentally realistic intake of cadmium on calcium, magnesium and phosphate metabolism in bank voles, *Clethrionomys glareolus*. *Arch. Environ. Contam. Toxicol.* **29**, 180–186.

TX015521U